JMEPEG (2006) 15:463-467
DOI: 10.1361/105994906X117314

1059-9495/$19.00

Assembling Single Cells to Create a Stack: The Case of a 100 W Microtubular Anode-Supported Solid Oxide Fuel Cell Stack

Nigel M. Sammes, Roberto Bove, and Yanhai Du

(Submitted January 16, 2006; in revised form May 22, 2006)

Microtubular solid oxide fuel cell systems have many desirable characteristics compared with their planar counterparts; however, there are many obstacles and difficulties that must be met to achieve a successful and economically viable manufacturing process and stack design. Anode-supported tubes provide an excellent platform for individual cells. They allow for a thin electrolyte layer, which helps to minimize polarization losses, to be applied to the outside of the tube, thus avoiding the difficulty of coating the inside of an electrolyte or cathode-supported tubes, or the stack design problem of having a fuel chamber if the anode is on the outside of the tube. This article describes the fabrication of a traditional (Ni-YSZ) anode tube via extrusion of a plastic mass through a die of the required dimensions. The anode tubes were dried before firing, and tests were performed on the tubes to determine the effects of prefiring temperature on porosity. The porous tubes had a vacuum applied to the inside while being submerged in aqueous electrolyte slurry. Various parameters were examined, including vacuum pressure, submergence time, and drying conditions, and were studied using microscopy. Cathode coatings (based on both doped lanthanum manganite and doped lanthanum cobaltite) were applied using a brush-painting technique, and were optimized as a function of paint consistency, drying conditions, and firing temperatures. The finished tubes were then stacked in an array to provide the specific current/voltage requirements, using a brazing technique. This article will describe the output characteristics of a single cell and a small stack (of 100 W designed power output).

Keywords anode support, brazing, extrusion, solid oxide fuel cell (SOFC), stack

1. Introduction

Solid oxide fuel cells (SOFC) represent an emerging technology for clean, reliable, and flexible power production. The main advantages of power production through SOFCs are the high conversion efficiency, the absence of combustion, and the fuel flexibility that allows a variety of fuels (including those derived from renewable sources) to be used. There is a copious amount of literature describing in detail the advantages and applications of SOFCs (Ref 1-7).

The first SOFC developed presented an operating temperature in the range of 900 to 1000 °C. Siemens-Westinghouse (Ref 8) and Rolls Royce (Ref 9) are still developing SOFCs to operate in that range of temperature, while a lot of research is now focused on reducing the operating temperature for solving the sealing and cracking problems related to SOFC operation (Ref 10-13).

There are two main SOFC configurations: tubular and planar. Planar SOFC performance is theoretically higher than that of tubular performance due to the reduced in-plane ohmic resistance. In addition, tape casting and other mass production techniques, for example, plasma spraying, can easily be applied for planar SOFC production, thus making possible a substantial production cost reduction. On the other hand, the tubular SOFC (TSOFC) configuration, due to its geometry, is capable of solving the problems related to cracking, thermocycling, start-up time, and sealing. Table 1 summarizes the main characteristics of the two configurations.

The selection of suitable materials and the development of specific techniques for TSOFC construction have been described in previous publications by the authors (Ref 14-18).

In the current study, a 100 W stack design and construction are presented. The stack is composed of microtubular, anode-supported SOFCs. Problems related to the performance variation of a single cell, when embedded in a stack, are also identified.

2. Stack Configuration

While planar SOFCs are stacked to form a pile of cells, tubular stacks must be assembled in a different configuration.

Table 1 Characteristics of tubular and planar solid oxide fuel cells

Characteristic	Tubular	Planar
Power density	Low	High
Volumetric power density	Low	High
High-temperature sealing	Not necessary	Required
Start-up cool down	Faster	Slower
Interconnect	Difficult	High cost
Manufacturing cost	High	Low

This paper was presented at the ASM Materials Solutions Conference & Show held October 18-21, 2004 in Columbus, OH.

Nigel M. Sammes and **Roberto Bove,** Mechanical Engineering Department, and **Yanhai Du,** Connecticut Global Fuel Cell Center, University of Connecticut, Storrs, CT. Contact e-mail: sammes@engr.uconn.edu.

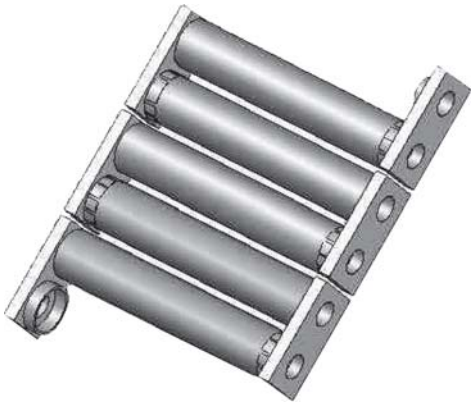

Fig. 1 PMAs

An easy way to arrange single cells is to align them, to form a planar multicell array (PMA) and then to stack the PMA as if it were a planar cell (Ref 19). The result is that stacks of different sizes can simply be fabricated by assembling different numbers of PMAs. In Fig. 1, a PMA is depicted. As further explained, the anode represents the internal layer of the tube, while the external surface is the cathode. As a consequence of this configuration, oxidant (air) and fuel can be easily managed and the external leakage is mostly limited to air mass loss.

In Fig. 2, a cross section of a PMA is schematically represented. As can be observed, possible leakages are likely to occur from the environment surrounding the tubes (limited by a box) and the external environment.

In the configuration of Fig. 2, however, air surrounds the stacked tubes, while fuel flows internally along the tubes; thus, the fuel leakage can occur only at the tube extremity. A good brazing between the current collector and the tube, however, is needed to avoid fuel leakage. Before the stack is assembled, tests are conducted to ensure that the joint preserves the stack from fuel leakage.

Figure 3 depicts the current collector. As can be observed, the two cylinders of the current collector are designed so that one is in contact with the inner part of the cell (i.e., the anode), and the other with the outer (i.e., the cathode); thus, every contiguous cell of the PMA is connected in series. Every PMA is then connected in series or parallel, according to the desired current and voltage characteristics.

3. Single-Cell Construction

The TSOFC can be externally supported using a porous media or can be supported by one of the fuel cell components itself (self-supported) (Ref 20). According to the supporting part, a self-supported fuel cell can be supported by an anode, cathode, or electrolyte. For the stack construction, based on our previous work (Ref 14), an anode-supported fuel cell has been selected. The supporting anode tubes are made of nickel (Ni) and yttria-stabilized zirconia (YSZ), coated with a thin YSZ electrolyte and a thin coat of lanthanum strontium magnate/cobaltite (LSM) cathode (Ref 14). Figure 4 represents the single-cell fabrication process. All information relative to tube fabrication procedures is extensively reported in Ref 14. After the construction process is complete, tubes are cut to a length of 110 mm. Figure 5 is a picture of the single fuel cells (Ref 14).

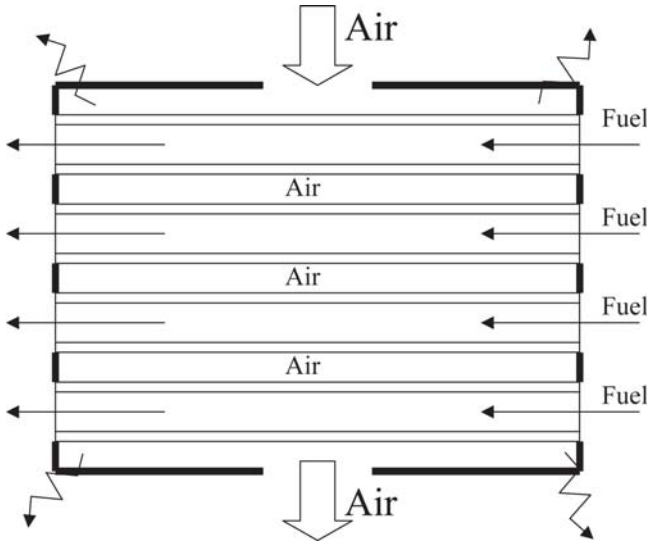

Fig. 2 Schematic cross section of a PMA

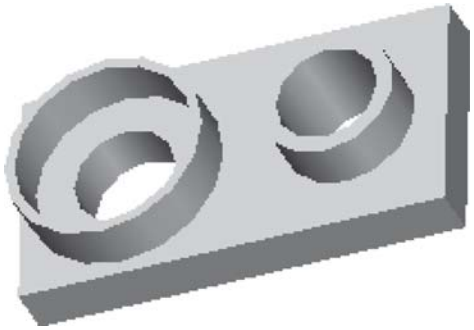

Fig. 3 Current collector

4. Joining Current Collectors and Single Cells

Current collectors are joined to the single cells using a brazing technique. An important issue for the joint integrity is the possibility of internal stress due to the different thermal expansions of the fuel cell components, the brazing material, and the current collector. For this reason, materials selection for stacking the cells is crucial. The thermal coefficient of expansion of the tube is estimated to be 12×10^{-6} K^{-1} (Ref 21). The material selected for the current collector is Ni200 (Ni 99.5%, Fe 0.15%, and Cu 0.05%), the coefficient of thermal expansion of which is 14×10^{-6} K^{-1} (Ref 22). The selection of the brazing material is dictated by the need of a compatible coefficient of thermal expansion and a melting point that is lower than that of the tube and the current collector. Pure Ag presents a melting point of 961.78 °C and a coefficient of thermal expansion of 18.9×10^{-6} (Ref 23); thus, it is an ideal candidate as a brazing material.

Silver braze metal in wire form (0.254 and 0.762 mm diameter, respectively) is placed in the gap between the tube outer diameter (OD) and the cap inner diameter (ID) at the base of the tube. The interface between the tube OD and the cap ID is designed with enough clearance so that the anode tube and the Ag wire fit tightly into the Ni end cap. This gap (0.254 mm) makes it possible for the molten Ag to flow around and fill the joint volume without overflowing. The lap depth required for brazing is calculated using the following relation (Ref 24):

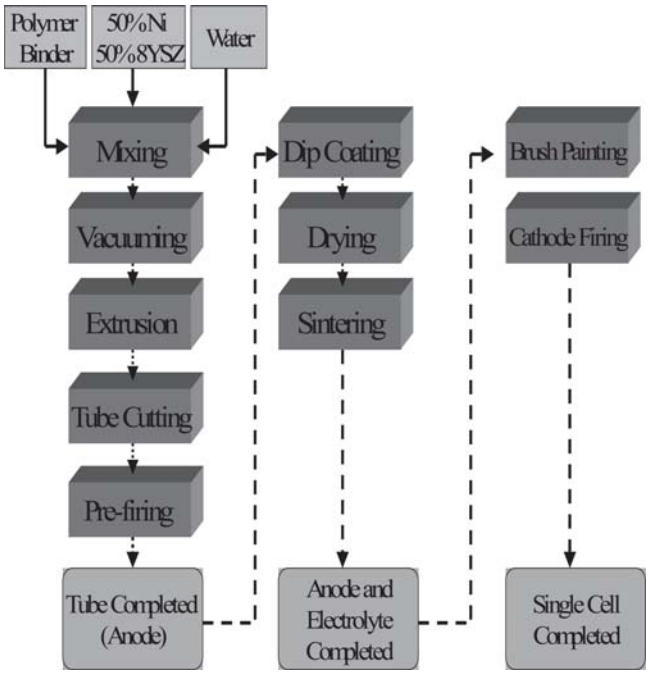

Fig. 4 Single cell production process

Fig. 5 Picture of the single cells (Ref 14)

$$X = \frac{W \cdot (D - W) \cdot T}{C \cdot L \cdot D} \quad \text{(Eq 1)}$$

where W, D, and T are the wall thickness, OD, and tensile strength of the anode tube, respectively; C is the joint integrity factor with a value of 0.8; L is the shear strength of the Ag braze alloy; and X is the lap depth. The brazing process takes place in a furnace, in specific environmental conditions (i.e., in the presence of a slightly reducing/inert atmosphere of 98% Ar and 2% H_2) and under the temperature profile of Fig. 6. These conditions are set for avoiding the oxidation of Ni and Ag, thereby enhancing the mechanical and the electrical performance of the joint. As seen from Fig. 6, the temperature is ramped up to 800 °C at a rate of 40 °C/min, and again ramped to 900 °C at 6 °C/min (to avoid excessive overshoot temperature), and is held at that temperature for approximately 15 min. This provides enough time for the assembly to come to thermal equilibrium. The temperature is then ramped up at 10 °C/min to 1100 °C (the brazing temperature) and allowed to soak for 6 min. The assembly is then cooled at 10 °C/min to 900 °C and allowed to equilibrate for 15 min. It was then cooled at 3 °C/min to room temperature.

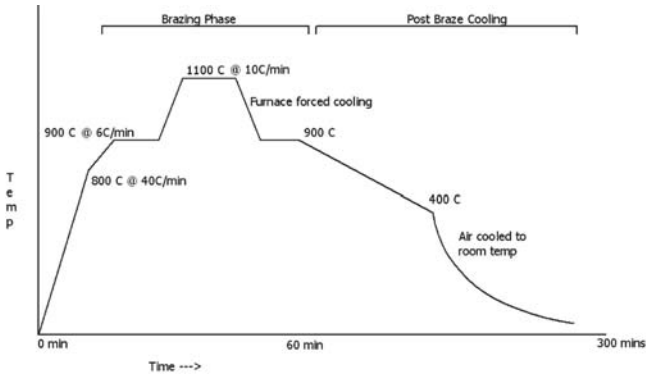

Fig. 6 Brazing temperature profile

Table 2 Tests results on joint samples

Sample ID	Leakage	Conductivity, ms	Torque, kNm	Microstructure
1	Yes	0-1	0.003	Nonuniform
2	No	4	0.0158	Uniform
3	No	5	0.0160	Uniform

Before assembling the stack, sample joints were realized to perform mechanical, leakage, and conductivity tests. Microscopic analysis is also conducted to check the uniformity of the joint. The results of these tests allowed the brazing procedure to be optimized, as described in Ref 24. Table 2 briefly shows the optimization history.

The sample results are reported in Table 2 in chronological order, thus showing the improvements obtained due to each test feedback. As can be seen, the maximum conductivity achieved is about 5 ms, and the nominal failure torque is about 0.016 kNm.

The microscopic analysis of the improved joint (sample ID 3 in Table 2) is reported in Fig. 7 (Ref 24). As can be seen, there is very good wetting of both the Ni metal tube and the SOFC anode tube. Silver is observed to diffuse into the ceramic surface as shown in Fig. 7(a) and (b), and more distinctively in Fig. 7(c). The open porosity of the anode tube helped to facilitate the diffusion of Ag. From Fig. 7(c), it can be seen that the Ag has diffused about 50 μm into the ceramic surface.

5. Stack Design and Expected Performance

Before assembling the stack, tests on the single cells are performed. Although SOFCs can operate with a variety of fuels, hydrogen is considered in the current study. The tests are conducted in an electric furnace (i.e., under isothermal conditions). A constant inlet flow rate is provided to the cell, while current density is varied. First tests are conducted at 850 °C, repeated at 800 °C, and then at 750 °C. Finally, the tests are repeated again at 850 °C. Figure 8 shows the voltage variation during the tests, and Fig. 9 shows the relative power density.

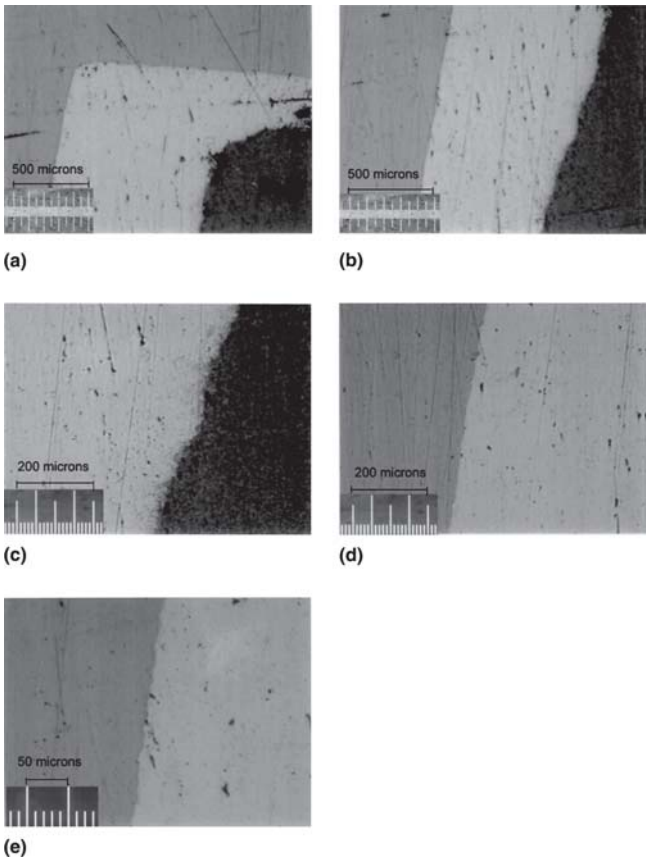

Fig. 7 Optical microscopy of the bond layer: (a) Ni-Ag-YSZ joint corner; (b) Ni-Ag-YSZ joint plane; (c) Ag-YSZ interface; (d) Ni-Ag interface; and (e) Ni-Ag interface at higher magnification (Ref 23)

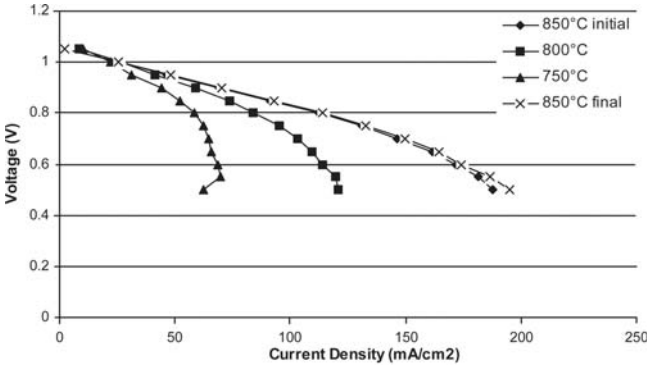

Fig. 8 Voltage-current density tests results at different temperatures and a constant inlet flow rate

It is clearly visible that a change in temperature leads to a remarkable performance variation. This behavior is not surprising, because it is well known that conductivity is connected to the operating temperature. Figures 8 and 9 also show that temperature cycling does not significantly influence the cell performance. As results of the tests, the operating temperature chosen for the stack is 850 °C. The fuel utilization relative to the tests shown in Fig. 8 and 9 is always below 20%; thus, additional tests have been performed at different flow rates. Flow rates equal to 25, 50, 75, and 100 mL/min are provided to the cell, and the current density is varied for each of them. The fuel utilization is computed as:

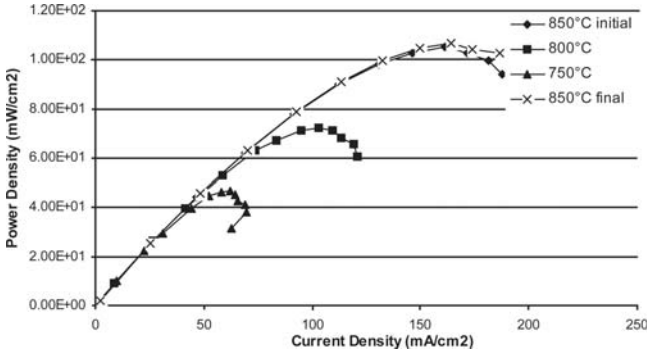

Fig. 9 Power density-current density at different temperatures and a constant inlet flow rate

$$u_f = \frac{I/(2F)}{n_{H_2,\,inlet}} \qquad \text{(Eq 2)}$$

where I is the electric current provided by the cell (expressed in amperes), F is the Faraday constant, and $n_{H2,inlet}$ is the hydrogen molar flow rate provided to the cell.

Figure 10 represents the result for the voltage and the relative fuel utilization variation. In Fig. 11, the relative power densities are depicted.

As fully explained in a previous study (Ref 25), once the performance of the SOFC is known, the choice of the optimal active surface value (i.e., in the current study, the number of single cells to be stacked) must be determined on an economic basis. If the stack, in fact, operates at high current density, a reduction of the investment cost is achieved. However, increasing the current density leads to an efficiency reduction (i.e., an increase in operating cost). The tradeoff between operating and investment costs determines the optimal size of the active surface. At the present time, however, SOFCs are still in an experimental phase, and the construction cost is a long way from that expected on the market. For this reason, the number of single cells to be stacked for realizing the stack is chosen on the basis of the maximum performance achieved by the single cells at reasonable values for the current density and fuel utilization.

The design point chosen is characterized by a current density of 119.3 mA/cm^2, a voltage of 0.5 V, and a power density of 59.5 mW/cm^2. The main characteristics of the stack are reported in Table 3. It should be noted that, once in operation, the stack will be tested under different conditions, and the optimal combination of operating parameters that guarantees good performance and stable conditions will be assessed. For this reason, the value of 100 W should not be considered nominal, but a reference condition.

Although the methodology developed for the single-cell fabrication and assembly showed promising results and allowed the stack to be fabricated, there are still some issues to be considered when passing from single cells to a complete stack. First, the single cells have been tested in an isothermal environment, and although the stack can operate under these conditions (i.e., inside a furnace), when a complete system is assembled the isothermal condition ceases to exist. Second, due to the configuration of the current collectors, in-plane ohmic losses can be quite high, thus reducing the overall performance. For a better understanding of this phenomenon, a two-dimensional model of the TSOFC has been implemented and solved using the commercial software FEMLAB (Comsol, Inc.,

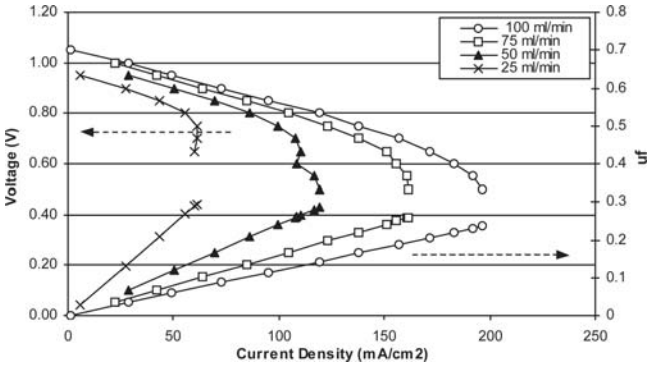

Fig. 10 Voltage variation and relative fuel utilization for different inlet flow rates

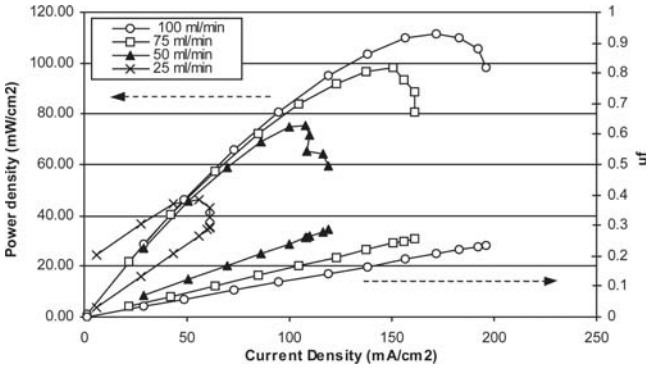

Fig. 11 Power density variation and relative fuel utilization for different inlet flow rates

Table 3 Main characteristics of the stack at reference condition

Characteristic	Value
Power	100 W
Fuel utilization	~30%
Current density	120 mA/cm^2
Power density	59.64 mW/cm^2
Single-cell diameter	1.32 cm
Single-cell length	11 cm
Electric current	5.44 A
Number of single cells	40
Stack voltage	20 V

Burlington, MA). The first results (Ref 19) show that the current runs mostly along the cylinder surface rather than perpendicularly from one electrode to the other. This causes a relevant performance reduction. Additional simulation results on a single cell can be found in another publication by the authors (Ref 19).

6. Conclusions

In the present article, the work for designing and constructing a 100 W micro-TSOFC is illustrated. The realization of the stack is the result of years of interdisciplinary work focused on single-cell construction, brazing technique development, numerical simulations, and the direct experience of the authors. The stack is composed of 40 single cells, connected through current collectors in PMA configurations. Further tests on the stack will be conducted to find possible stack improvements and optimal operating conditions.

References

1. J.P. Strakey, M. Williams, W.A. Surdoval, and S.C. Singhal, U.S. DOE Solid Oxide Fuel Cell Program, *Proceedings of Sixth European Solid Oxide Fuel Cell Forum,* European Fuel Cell Forum, Lucerne, Switzerland, 2002, Vol. 1, p 48-59
2. G.A. Tompsett, C. Finnerty, K. Kendall, T. Alston, and N.M. Sammes, Novel Applications for Micro-SOFCs, *J. Power Sources,* 2000, **86,** p 376-382
3. S.C. Singhal, Advances in Solid Oxide Fuel Cell Technology, *Solid State Ionics,* 2000, **135,** p 305-313
4. M. Dokiya, SOFC System Technology, *Solid State Ionics,* 2002, **152-153,** p 383-392
5. H. Tu and U. Stimming, Advances, Aging Mechanisms and Lifetime in Solid-Oxide Fuel Cells, *J. Power Sources,* 2004, **127,** p 284-293
6. E G & G Technical services, Inc., *Fuel Cell Handbook,* 6th ed., U.S. Department of Energy, 2002
7. J. Larminie and A. Dicks, Fuel Cell Systems Explained. London, UK: J. Wiley and Sons, LTD, 2000
8. S. Vora, "Small-Scale Low Cost SOFC Power System," Paper presented at the SECA Annual Workshop and Core Technology (Boston, MA), Department of Energy and NETL, May 2004
9. G. Agnew and A. Spangler, 2004, "Reducing Fuel Cell System Costs without Lowering Operating Temperature," Paper presented at the 2nd International Conference on Fuel Cells Science Engineering and Technology (Rochester, NY), ASME, June 2004
10. P. Banace, N.P. Brandon, B. Girvan, P. Holbeche, S. O' Dea, and B.C.H. Steele, *J. Power Sources,* 2004, **131,** p 86-90
11. J. Love and R. Ratnaraj, Operation of CFCL's All-Ceramic Stack Technology, *Proceedings of Sixth European Solid Oxide Fuel Cell Forum,* European Fuel Cell Forum, 2004, Vol. 1, p 355-362
12. K. Ogasawara, Y. Baba, K. Fujita, H. Kameda, H. Yakabe, Y. Matsuzaki, and T. Sakurai, Development of Anode Supported Planar SOFC with Metallic Interconnectors Operated at Reduced Temperature, *Proceedings of Sixth European Solid Oxide Fuel Cell Forum,* European Fuel Cell Forum, 2004, Vol. 1, 2004, p 394-400
13. B. Zhu, Functional Ceria-Salt-Composite Materials for Advanced ITSOFC Applications, *J. Power Sources,* 2003, **114,** p 1-9
14. Y. Du and N.M. Sammes, *J. Power Sources,* 2004, **136,** p 66-71
15. Y. Du, "Fabrication and Characterization of Micro-Tubular Solid Oxide Fuel Cells," Ph.D. dissertation, University of Waikato, 2004
16. Y. Du and N.M. Sammes, Fabrication and Properties of Anode Supported Tubular Solid Oxide Fuel Cells, *J. Eur. Ceram. Soc.,* 2001, **21**(6), p 727-735
17. Y. Du, N.M. Sammes, and G.A. Tompsett, Fabrication of Tubular Electrolytes for Solid Oxide Fuel Cells Using Strontium and Magnesium Doped $LaGaO_3$ Materials, *J. Eur. Ceram. Soc.,* 2001, **20**(7), p 959-965
18. Y. Du, N.M. Sammes, G.A. Tompsett, D. Zhang, J. Swan, and M. Bowden, Extruded Tubular Strontium and Magnesium-Doped Lanthanum Gallate, Gadolinium-Doped Ceria, and Yttria Stabilized Zirconia Electrolytes, *J. Electrochem. Soc.,* 2003, **150,** p 74-A78
19. R. Bove, N.M. Sammes, and P. Lunghi, "Design of a Tubular SOFC Stack Aided by Numerical Simulations," Paper presented at Fuel Cell Seminar 2004 (San Antonio, TX), Fuel Cell Seminar Organizing Committee, Nov 2004
20. N.Q. Minh and T. Takahashi, Science and Technology of Ceramic Fuel Cells, Amsterdam: Elsevier, 1995
21. A.V. Durov, B.D. Kostjuk, A.V. Shevchenkoand, and Y.V. Naidich, Joining of Zirconia to Metal with Cu-Ga-Ti and Cu-Sn-Pb-Ti Fillers, *Mater. Sci. Eng.,* 2000, **A290,** p 186-189
22. W.B. Hanson, K.I. Ironside, and S.A. Fernie, Active Metal Brazing of Zirconia, *Acta Mater,* 2000, **48,** p 4673-4676
23. D.R. Lide, *CRC Handbook of Chemistry and Physics,* 77th ed., Boca Raton, FL: CRC Press, 1996
24. A. Basak, R. England, and N.M. Sammes, Determination of the Mechanical integrity of Ceramic-to-Metal Braze Joints in SOFC Interconnect Applications, *Proceedings of Sixth European Solid Oxide Fuel Cell Forum,* European Fuel Cell Forum, Lucerne, Switzerland, 2004, Vol. 2, p 950-959
25. R. Bove and N.M. Sammes, Optimal SOFC Size Design for Minimal Cost of Electricity Achievement, Fuel Cells Science and Technologies, ASME, 2005, Vol. 2, p 9-14